Experimental investigation of air-water two-phase flow in a 1mm x 1mm cross section channel

Final version of the full paper for the presented ECCE-6 abstract

Rahel G/W Negera[1], Bernd Wittgens[2], Lars R. Sætran[1] and Paal Skjetne[2]

[1]*Department of Energy and Process Engineering, Norwegian University of Science and Technology, Trondheim, Norway*
[2] *Department of Process Technology, SINTEF Materials and Chemistry, Trondheim, Norway*

Abstract

In chemical industries, gas-liquid two phase flows with very low liquid loading are common. One area involving gas-liquid flow with low liquid loading is miniaturized channels for the design of structured catalyst bed as opposed to conventional packed bed catalytic reactors. Models for mass transfer and reaction kinetics depend on accurate identification and characterization of the two-phase flow pattern. In this paper an investigation of air-water flow pattern in a horizontal 1mm x 1mm PMMA (Polymethyl Methacrylate) square channel is presented. The water and air flow rate ranges from 0.02 ml/min – 1ml/min and 4 ml/min – 250 ml/min, respectively. The flow patterns are visualized using a high speed CCD camera mounted on a microscope. The camera is capable of taking up to 1000 frames per second. Further, the two-phase flow pattern is mapped using the superficial velocities of water (Vsw) versus superficial velocity of air (Vsa). Flow patterns for different entrance conditions are compared. In addition, the flow at two 90° bends at 1 mm distance from each other is investigated.

Keywords: gas-liquid flow, two-phase flow, flow in small channel

1. Introduction

Two-phase gas–liquid flow in chemical equipments has been used in conventional size flow channels for years. The flow patterns which describe the mass transfer and reaction kinetics in the modeling and design of such equipment has been well studied for practical flow conditions. However, miniaturization is becoming an issue for many applications where the limiting factor is interfacial area, such as mass transfer and reaction kinetics of catalytic reactors. Two-phase flow transport phenomena in miniaturized channels can be quite different from those in conventional ones since the

flow can be governed surface/interfacial forces. The effect of such forces on conventional channel flow is negligible. Furthermore, the effects of geometry are more pronounced in such small channels. The behavior of bubbles and slugs in a confined rectangular cross section has been observed to be different from that in unconfined circular cross section. It is however more convenient and economical to produce miniaturized equipments with rectangular channels than circular ones. A prominent feature of miniaturized equipment is the large surface to volume ratio. Very long channels are packed into very small volumes (chips). This is achieved by use of meandering channels, thus straight channels are separated by 180 degree turns that are either semi circular or consist of two consecutive 90 degree square bends. Thus, this study is focused on investigation of gas-liquid two-phase flow in square channels with 90 degree bends.

In this study, air–water two-phase flow in a 1mm x 1mm cross sectional channel made of PMMA (Polymethyl Methacrylate) is investigated. The flow patterns obtained are compared with other works to analyze how the flow pattern changes as the channel size is decreased from the order of several centimeters, down to millimeters and micrometers. In addition, the effect of 90 degree bends on the pattern is investigated.

2. Background

Gas-liquid flows are widely used in a variety of industrial processes. The study of flow pattern in two-phase flow helps to qualitatively understand the flow and leads to better prediction methods for the various two-phase flow parameters like pressure drop, mass and heat transfer coefficients, void fraction, etc which are important in the design of process equipment. The two phase mixtures in these processes are usually multi-component and component mass transfer is often a limiting factor performance of the process. The mass transfer process in mixing of different phases is well developed for conventional size channels. The flow pattern most suitable for predicting effective mixing process is a uniform thickness film flowing along the channel wall. The film theory explains that mass transfer in such a case occurs only by diffusion through the laminar layer near the wall. Here the concentration gradient determining the mass flux is almost linear. The flow in small channels is usually laminar so the mass transfer is only by diffusion. So flow patterns creating wall films can easily be used in the investigation of reactions in miniaturized reactors.

Fluid flow patterns in conventional flows are relatively well studied. However recent industrial developments towards miniaturization of channels call for a focus on the study of two phase flows in confined geometries. In such geometries, interfacial phenomena which are negligible in conventional flow play the dominant role. The relative importance of different forces on the flow patterns can be examined using dimensionless numbers.

Different classifications have been proposed for the distinction between conventional or normal size channels, mini channels and micro channels. Some of the proposals give fixed dimensions for classification regarding specific engineering equipment and others give correlations which are dependent on physical properties of the fluid.

Among the first were Shah(1986) and Mehendale et. al (2000) who gave the discerning size between small and normal sized for heat exchangers as 6mm. Furthermore, they classified sizes below 100μm as micro, sizes between 100 μm and 1 mm as Meso and sizes between 1 and 6 mm as compact. Kandlikar (2001, 2002) classified the channels used in the field of microelectronics and micro-electro-mechanical-systems (MEMS) as conventional channels for sizes greater than 3mm, mini channels for sizes between 200 μm and 3mm, and micro channels for sizes between 10 and 200μm. Among the groups who presented correlations dependent on the physical properties of the fluid as a characteristic dividing line of the size classification are Brauner and Moalem-Maron(1992). They derived the criterion in terms of the Eotwös number, Σ (also represented by Eö and Eo), to be greater than 1 in the region where surface tension is the dominant force compared to gravity.

$$\Sigma = \frac{4\pi^2 \sigma}{\left(\rho_l - \rho_g\right)D_h^2 g} > 1 \qquad (1)$$

More commonly the so called Bond number, Bo, is used to characterize the ratio between gravitational and interfacial forces, i.e. in essence the inverse of the Eotwös number, but without the scaling factor of $4\pi^2$:

$$Bo = \frac{\rho g D_h^2}{\sigma} < 4\pi^2 \qquad (2)$$

Tripplett et al (1999) categorized channels with hydraulic diameter less than or equal to the Laplace constant (L) as small channels. The Laplace constant (L, with dimension meters) is defined as

$$L = \sqrt{\frac{\sigma}{g\left(\rho_l - \rho_g\right)}} \qquad [m] \qquad (3)$$

Kew and Cornwell (1997) also defined the dimensionless Confinement number (Co) based on the Laplace number for classifying the channels where the effect of confinement is significant for channels with the following condition.

$$Co = \frac{1}{D_h} \sqrt{\frac{\sigma}{g(\rho_l - \rho_g)}} > 0.5 \qquad (4)$$

The parameters used in this study give the values for Σ, L and Co to be 149, 0.0019 and 1.95, respectively. In all the three cases air-water two-phase flow in a 1mm x 1mm channel can be classified as surface tension dominated. Nevertheless, we are operating in a transition regime where gravitational force still has an effect. However, it does not account for the effect of the channel material. In general one has to account for the surface energies of both liquid/vapor, solid/vapor and solid/liquid interfaces. It was observed that the surface energy between the liquid (water) and the solid surface of the PMMA channel had an effect on the flow regime. Theoretically PMMA has a contact angle of 70° when it is first exposed to water. Thus, water partially wets PMMA. However, it tends to become more hydrophilic the longer it is exposed to

water. This behavior of PMMA is reported by Wang et al. (2001). The effect of wall properties on the flow patterns has been reported by Hewitt and Angeli (2000) which investigate the flow pattern of oil-water two-phase flow in one inch diameter pipes made of steel and acrylic resin, respectively. Therefore, it is inadequate to classify channel sizes based on assumptions which do not include; the surface energy between the system components, surface roughness and channel geometry. Even so, we would like to compare the flow patterns observed experimentally in this work with observations from work done on channels ranging from meters to micrometers.

Hewitt (1978) explained the different flow regimes encountered for gas-liquid flowing in horizontal *normal* size channels. For such channels gravitational forces are important displacing the liquid towards the bottom of the channel. For *compact* channels, Fukano and Kariassaki (1993) reported that the effect of gravity on flows in capillary tubes of diameters less than 5mm is negligible. They tested vertical downward and upward flows and horizontal flow and concluded that the direction of flow does not matter in such scales. The flow pattern maps for horizontal gas-liquid two-phase flow in *conventional* size channels presented by Mandhane et. al (1974) is considered here to represent the flow pattern in sizes in the order of several centimeters. Triplett et al (1999) used air-water two-phase flow to investigate the flow pattern of gas-liquid flow in circular and semi triangular channels. The hydraulic diameters of the channels were 1.1 and 1.45 mm for the circular cross section and 1.09 and 1.49 mm for the semi-triangular cross section. The ranges of the superficial velocities for the gas and liquid were 0.02 – 80 m/s and 0.02 – 8 m/s, respectively. The flow pattern presented here is in good agreement with the results presented in their work. For the case in the order of micro meters, the work of Serizawa et al. (2002) is taken. They performed flow pattern mapping for circular silica micro channels of ID 20, 25 and 100 µm in the flow ranges of superficial liquid velocity of 0.0032 – 17.5 m/s, and superficial gas velocity of 0.0022 – 295.3 m/s.

The effect of cross-sectional geometry on flow pattern has been reported by G. Wölk et al. (2000). The investigation was done on air-water two-phase vertical flow in channels of hydraulic diameter of 6mm for the ranges of both gas and liquid superficial velocities from 0.1 to 10 m/s. The three flow patterns observed in these ranges are slug, dispersed bubble and churn flow. The comparison is carried out between one circular channel and four different non-circular channels (with rectangular, rhombic, and equilateral triangular cross-section). The transitions between the three patterns are presented for all the cross-sections. Comparing the circular with the rectangular channel (aspect ratio = 0.97), the transition lines from slug flow to dispersed flow, and from dispersed flow to churn flow occur at lower superficial velocities for the rectangular channel. Moreover, the transition from slug flow to churn flow occurs at slightly lower superficial gas velocity for the rectangular channel. The main reason given to these shifting of the transitions is the turbulent secondary flow occurring in non-circular channels and the steeper radial distribution of the phases and/or velocities. In the work of Triplett et al (1999), flow patterns of air-water two-phase flow in circular and semi-triangular (triangular with one corner smoothed) are investigated for hydraulic diameters of 1.1 and 1.45 mm for both cross-sections. The gas and liquid superficial velocities covered are 0.02 – 80 m/s and 0.02 – 8m/s, respectively. The patterns observed in these ranges are slug, Slug-Annular, bubbly, and churn in all the cases. Comparing the transition lines between the patterns

for the different cases, there is no significant shift which could specifically reflect the effect of geometry.

3. Experiment

The schematic representation of the experimental setup is shown in Figure 1. The channels used in the investigation were mechanically milled on a 40 mm x 90mm PMMA plate of 6mm thickness. A cover was made of the same material with 2mm thickness, with holes for the inlet and outlet of the flow. The cover was bonded to the base plate using the solvent bonding method proposed by Klank, et. al (2002). In this method, the PMMA plates are immersed in an ethanol bath for 10 minutes, before the ethanol is wiped off by lint-free tissue to remove excess ethanol. The two plates are then pressed together by a mounting press and baked in a laboratory oven for 90 minutes at 100 ^{o}C. Then they are left to cool down while they are still pressed together. Later connectors are glued to the inlet and outlet holes. The channel designs used in the investigation are shown in Figure 2. The channel size of the test section is 1mm x 1mm square in all the three cases.
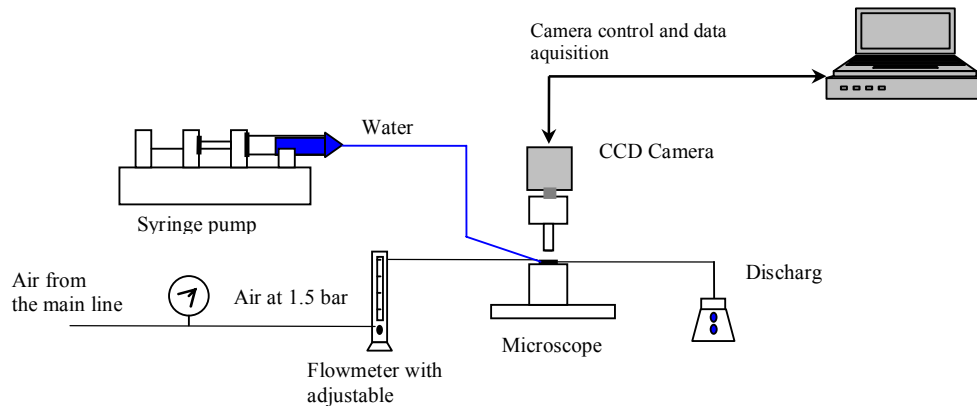
Figure 1: Schematic representation of the experimental setup.

Air from the main line enters the pressure vessel and is controlled to enter the test section at 1.5 bar. The flow rate of air is controlled by a rotameter with adjustable flow rate. Water, mixed with coloring material to make the flow visualization easier, is driven by a syringe pump (PHD 2000; Harvard Apparatus). The two streams are injected to the test section, water from the left/upper branch and air from the right/lower branch, where the flow rate of air is increased at different steps to cover the test range for a fixed flow rate of water. The exit pressure is almost atmospheric. The visualization of the flow pattern was realized through a microscope (BX51, Olympus) with 4x magnification objective. The images are recorded by a high speed CCD camera (Photron FastCam) mounted on the microscope. The camera has a recording speed up to 1000 frames per second with 1024 x 1024 resolutions and shutter speed down to 1/ 220000 s. The two- phase flow was visualized at the

entrance to the test section and again at a position 30-40mm downstream. The later position was used when mapping the flow pattern. In addition, the two-phase flow was visualized at the two 90° bends in the third channel design.
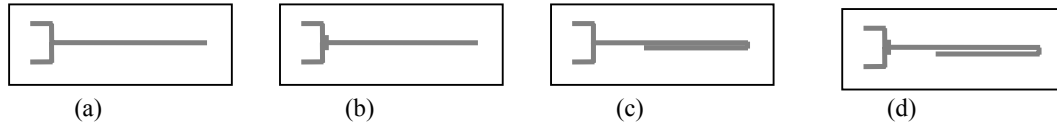
| (a) | (b) | (c) | (d) |

Figure 2. Channel designs (a) 90 degree entrance to the test section, (b) A 2mm x 2mm mixing zone before entrance to the test section, (c) Channel with 2 x 90° bends 1mm from each other, entrance the same as case (a), (d) Channel with 2 x 90° bends 1mm from each other, entrance the same as case (b).

Definitions of the dimensionless numbers which show the relative importance of different forces on the flow are given in Table 1. Table 2 summarizes the physical parameters used in the calculation of these dimensionless numbers. The ranges of air and water superficial velocities and values of dimensionless numbers covered in this experiment, and for the flow maps considered for comparison, are summarized in Table 3.

Table 1. Definition of the dimensionless numbers used in the comparison

Dimensionless numbers	Definitions	Formulae
Bond Number, *Bo*	Ratio of gravitational force to interfacial force	$\dfrac{\rho g D_h^2}{\sigma}$
Capillary Number, *Ca*	Ratio of viscous force to interfacial force	$\dfrac{\mu U}{\sigma}$
Knudsen Number, *Kn*	Ratio of mean free path of fluid molecules to characteristic length of flow channel	Gas: $\dfrac{\lambda}{D_h}$; Liquid: $\dfrac{\delta}{D_h}$
Peclet Number, *Pe*	Ratio of advection to diffusion effects	$\dfrac{D_h U}{D}$
Reynold Number, *Re*	Ratio of inertial force to viscous force	$\dfrac{\rho U D_h}{\mu}$
Weber Number, *We*	Ratio of inertial force to interfacial force	$\dfrac{\rho D_h U^2}{\sigma}$

Table 2. Physical parameters of the fluids in the flow

Parameters at 1 atm and 20 $^{\circ}$C	Water	Air
Density [Kg/m^3]	1000	1.2
Viscosity[Ns/m^2]	1.00×10^{-3}	1.79×10^{-5}
Surface tension [mN/m]	73	
Mean free path of air molecules [m]	1.00×10^{-7}	
Lattice spacing of water molecules [m]	1.00×10^{-10}	
Diffusivity of air in water [m^2/s]	1.70×10^{-8}	

As can be seen from the values of the dimensionless numbers in Table 3, the following can be said about the air-water two-phase flow in the 1mm x 1mm square channel;

- The value of *Kn* which is less than 0.001 indicates that the flow of both liquid and gas in the channel can be treated as continuum. Thus Navier-Stokes equation with no-slip boundary conditions can be used to describe the flow.
- The values of *Bo*, *Ca*, and *We* show that the effect of interfacial force is higher than the effect of gravitational force, viscous force and inertial force, respectively.
- The value of *Re* shows that the flow is laminar in the whole flow rate range and thus flow mixing is mainly by diffusion, and chaotic laminar mixing.
- The value of *Pe* is high indicating that mixing by diffusion and chaotic laminar mixing dominates. Thus the mixing can be compared to that in conventional sized flow ducts (Mandhane et al 1974).

Table 3. Summary of superficial velocity ranges and dimensionless numbers used in the different experiments

Experiments	Channel size	values	Superficial velocity[m/s] liquid	gas	Liquid loading [m³/MMm³]	Re liquid	gas	We	Bo	Ca	Kn liquid	gas	Pe
Serizawa et al. (2002)	20, 25 and 100 µm	Min.	0.0032	0.0022	1.1×10^{1}	0.064	0.003	2.8×10^{-6}	5.4×10^{-5}	4.4×10^{-5}	3.0×10^{-6}	1.0×10^{-3}	2.6
		Max.	17.5	295.3	8.0×10^{9}	1750	1980	4.2×10^{2}	1.3×10^{-3}	2.4×10^{-1}	1.5×10^{-5}	5.0×10^{-3}	1.7×10^{6}
This experiment	1 mm	Min.	0.0003	0.067	6.9×10^{1}	0.3	4.5	1.2×10^{-6}	1.3×10^{-1}	4.1×10^{-6}	3.0×10^{-7}	1.0×10^{-4}	3.9×10^{3}
		Max.	0.0167	4.33	2.5×10^{5}	16.7	279.4	3.8×10^{-3}		2.3×10^{-4}			2.5×10^{5}
Triplett et al.(1999)	1.09 mm	Min.	0.02	0.02	2.5×10^{2}	21.8	1.46	6.0×10^{-3}	1.6×10^{-1}	2.7×10^{-4}	2.8×10^{-7}	9.2×10^{-5}	2.5×10^{5}
		Max.	8.0	80	4.0×10^{8}	8720	5846	9.6×10^{2}		1.1×10^{-1}			5.1×10^{6}
Mandhane et. al (1974)	1.27 cm – 16.5 cm	Min.	0.003	0.03	2.0×10^{1}	38.1	25.5	1.6×10^{-3}	2.2×10^{1}	4.1×10^{-5}	1.8×10^{-9}	6.1×10^{-7}	2.2×10^{4}
		Max.	6.1	152.4	2.1×10^{8}	1.01×10^{6}	1.69×10^{6}	8.4×10^{4}	3.7×10^{3}	8.4×10^{-1}	2.4×10^{-8}	7.9×10^{-6}	1.5×10^{9}

4. Results and discussion

4.1. Flow in straight channel

The main flow patterns observed in the straight part of the channel are slug, annular, stratified wavy, wavy and churn flow. Table 4 summarizes the patterns observed and the corresponding entrance conditions. The water was colored using a red titer, thus appearing as a red/dark phase. The air phase appears as a yellow/light phase. The characteristics of the different patterns observed in this experiment are described as follows.

Slug flow

It is an intermittent flow of air slugs and liquid plugs. For a given water flow rate, the sizes of the air slugs and liquid plugs are usually evenly distributed at lower air flow rates then as the gas flow rate increases, their size range becomes larger.

Stratified wavy

The flow is separated to the "left/upper" and "right/lower" side walls (as seen when looking down the channel in the flow direction, i.e. from left to right in the figures). The liquid on the "left/upper" side wall is wavy which does not touch the "right/lower" side wall. In the case where there is no entrance mixing, for a given liquid flow rate the film on the "right/lower" side wall can be swept away at high gas flow rates. When there is a mixing area at the entrance, the liquid was more evenly distributed between the "right/lower" and "left/upper" sides.

Annular flow

The liquid films observed in this case are just on the "left/upper" and "right/lower" side corners and it looks stagnant. The thickness of the film on the two sides change as the gas flow rate increases. The liquid gas interface also becomes rougher as the gas flow rate is increased. For the case where there is no additional mixing area at the entrance, the liquid film at the right side can be swept away completely.
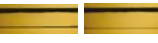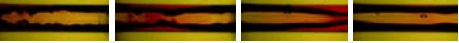
Wavy

The large amplitude waves of the liquid flowing at the "left/upper" side wall touches the film at the "right/lower" side wall which creates a kind of liquid ring that flows along the channel as a toroidal wave.

Churn

Breaking of liquid plugs creates waves and bubbles. This pattern is observed only for the case where there is an additional mixing area before the entrance to the test channel, e.g. Figure 2-b and 2-d.

Table 4. Summary of obserned flow patterns at the entrance and at 40 mm downstream.

Flow pattern	Entrance condition	Air-water flow at the entrance	Air-water flow at 40mm down stream
Slug	Direct Entrance		
	Entrance with 2x2mm mixing zone		
Annular	Direct Entrance		
	Entrance with 2x2mm mixing zone		
Wavy	Direct Entrance		
	Entrance with 2x2mm mixing zone		
Stratified Wavy	Direct Entrance		
	Entrance with 2x2mm mixing zone		
Churn	Entrance with 2x2mm mixing zone		

As shown in Figure3, the flow pattern obtained by Triplett et al. (1999) for an air-water two-phase flow in a 1.09mm diameter circular channel is compared with the data obtained in this work for a plain T-junction at the inlet. The data shows continuity even though the range of the flow rates in the two studies do not overlap. The flow pattern maps for the two entrance conditions considered are shown in Figure 4. As can be seen from the map, the transitions from slug flow to stratified wavy and wavy is similar for both conditions. However, transitions from annular to stratified wavy and then to wavy occurs at lower liquid flow rate in the case where there is a mixing area at the entrance. Furthermore, churn flow was observed only in the case when the 2x2mm mixing section was added to the inlet. Another difference observed between the two inlet configurations is that the annular pattern without liquid film on the "right/upper" side wall occurs at high gas flow rate when there is no additional mixing area at the entrance.

In Figure 5, the transition of patterns shown in the work of Mandhane et al.(1974) did not agree well with the flow pattern transitions we obtained. However, the wavy flow regions have matching areas. Again comparison has been done with data obtained for a plain T-junction at the inlet from this work.

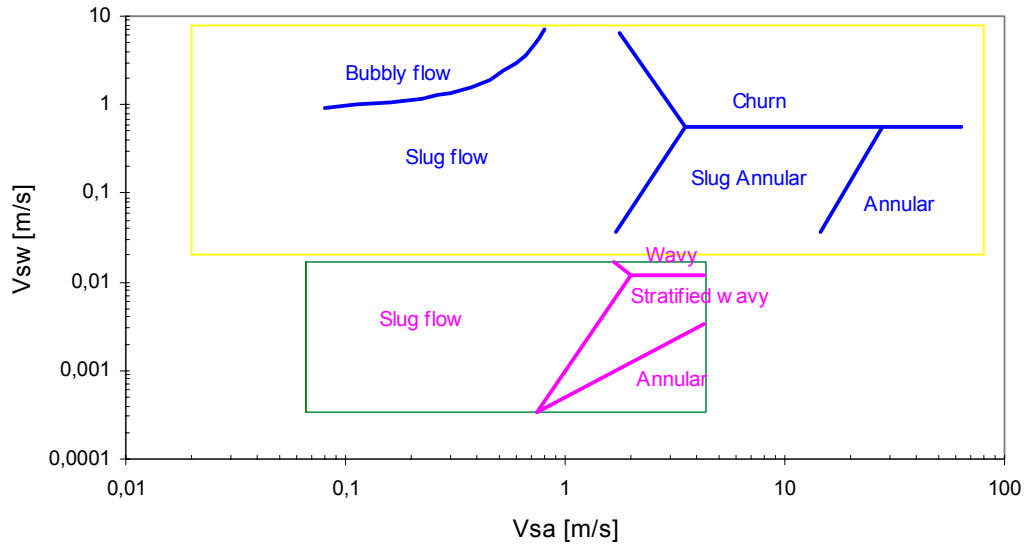**Flow pattern map comparison with Tripltt et al. (1999)**

Figure 3. Flow pattern map comparison with Triplett et al (1999), the area enclosed by yellow boundaries
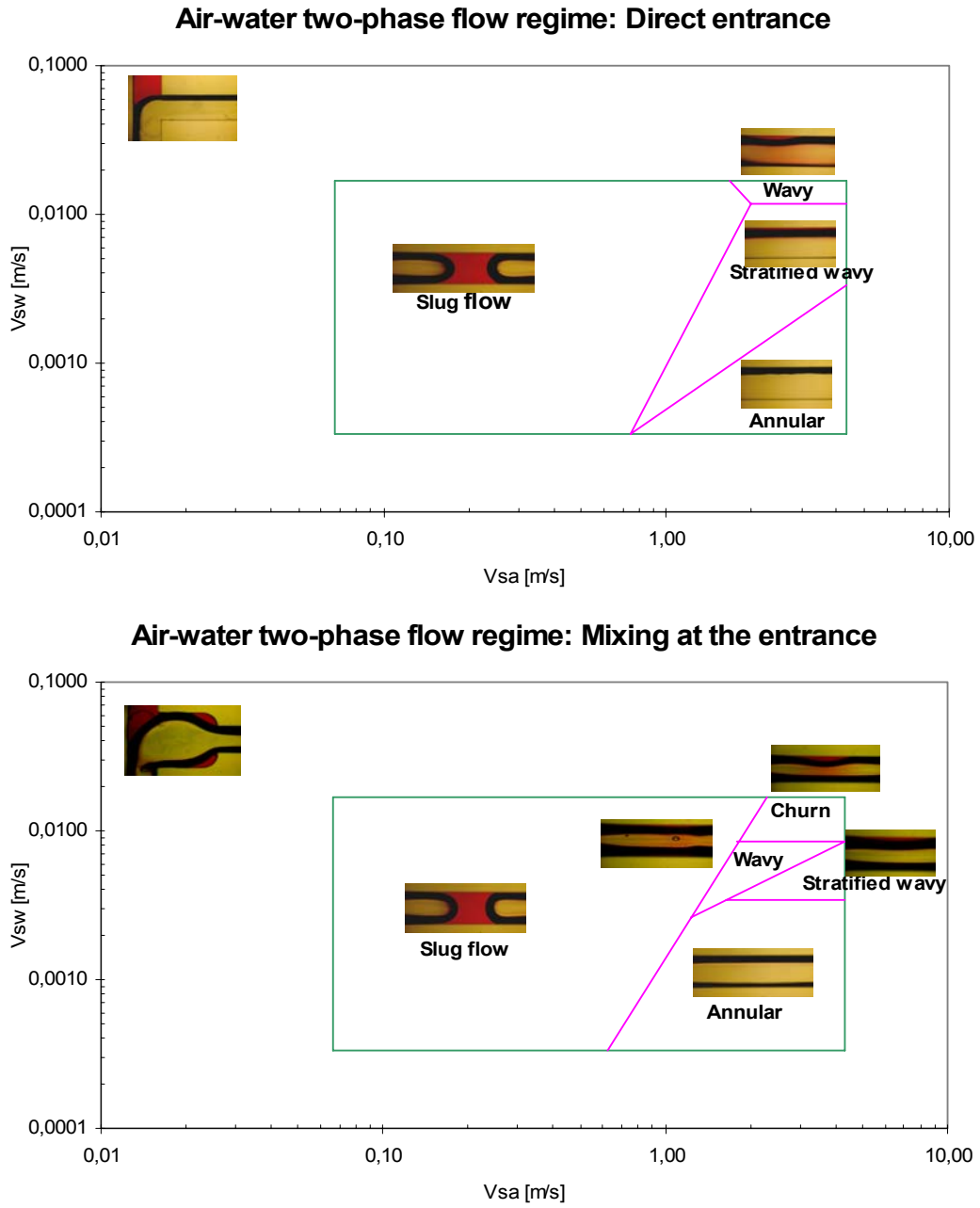
Air-water two-phase flow regime: Direct entrance

Air-water two-phase flow regime: Mixing at the entrance

Figure 4. Flow pattern maps obtained for the two entrance configurations.

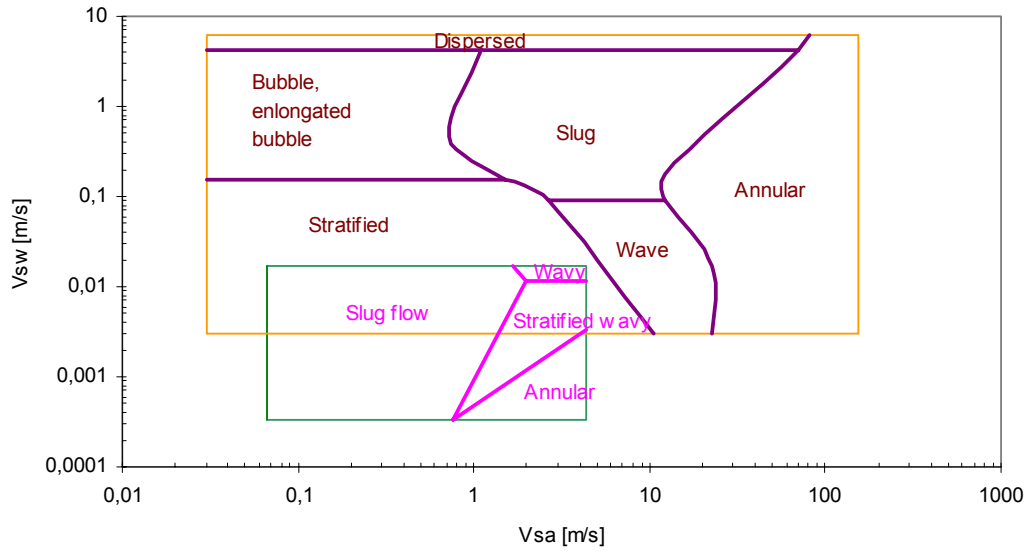**Flow pattern map comparison with Mandhane et al.(1974)**

Figure 5. Flow pattern map comparison with Mandhane et al. (1974), the area enclosed by orange boundaries.

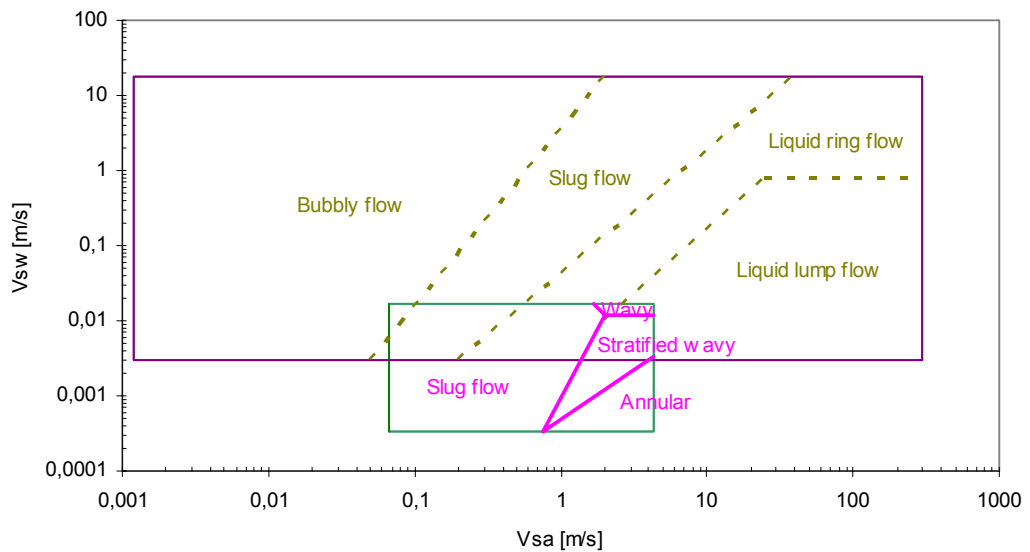**Flow pattern map comparison to Serizawa et al. (2002)**

Figure 6. Flow pattern map comparison with Serizawa et al. (2002), the area enclosed by violet boundaries.

The transition lines in the flow map of Serizawa et al. (2002), shown in Figure 6, is dotted since they are plotted based on the data points reported in the original work. The slug flow pattern shows continuity down to the flow rate ranges we investigated. In addition, the flow pattern classified as liquid ring flow in their report resembles with what we called wavy flow.

4.2. Flow in two 90 degree bends 1mm from each other

At the 90 degree bends, for a given liquid flow rate, the flow passes through the bends without changing its pattern at low gas flow rate. As the gas flow rate increases, the flow gets more deformed at the bend. This causes the formation of a new liquid plug at the second bend and/or pinch off of a passing air slug to create one or more bubbles. Thus a bubbly pattern is created here which was never observed in the section up stream the bend.

Examples of the main phenomena observed while the flow passes the bends are shown in Figure 7 below. In addition, the flow rate range where these different phenomena occur is plotted in the contour maps as shown in Figure 8 and Figure 9 for the two entrance conditions considered. In these maps, the flow outside the contour is not affected at the bend. In the area bound by the blue contour, new liquid plugs are created at the second bend. In the area bound by the red contour, air slugs break off at the bend creating one or more bubbles.

(a) Unchanged pattern (Vsw = 0.012 m/s, Vsa = 0.15m/s)

(b) New liquid plug forming at the second bend (Vsw = 0.002 m/s, Vsa = 0.75m/s)

(c) Air slug breaks off at the bend forming new bubble (Vsw = 0.017 m/s, Vsa = 0.75m/s)

Figure 7. Flow pattern observed at two 90 degree bends at 1 mm from each other.
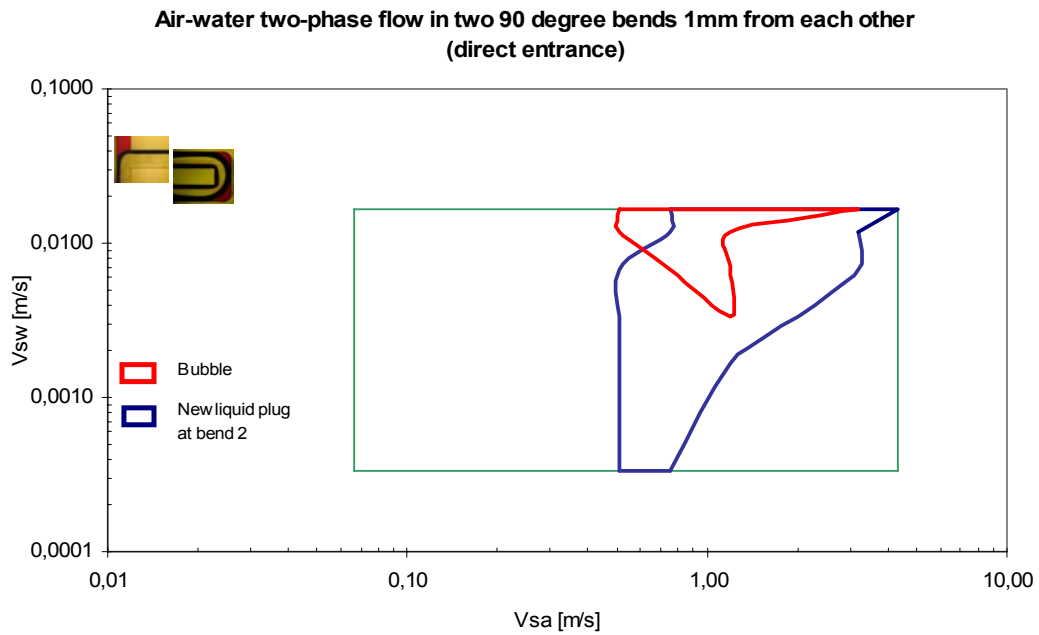
Figure 8. Contour map for the flow pattern observed at two 90 degree bends at 1 mm from each other for direct entrance condition
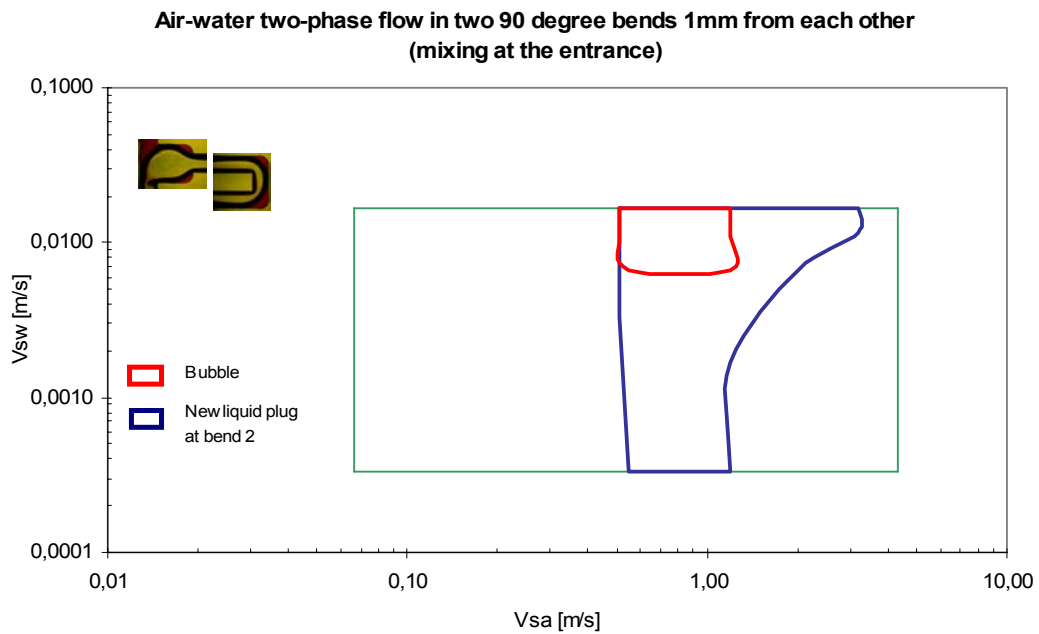

Figure 9. Contour map for the flow pattern observed at two 90 degree bends at 1 mm from each other for mixing at the entrance condition

5. Conclusion

In order to understand the flow of a gas-liquid two-phase flow in a 1mm x 1mm square cross section channel at low liquid loading, the flow patterns and their transition is experimentally determined for an air- water system. The water and air flow rates were in the ranges of 0.02 ml/min – 1 ml /min and 4 ml/min – 250 ml/min, respectively. Two different inlet designs were used to investigate the effect of mixing at the entrance on the flow pattern. In addition, changes to the flow pattern as the flow passed through two consecutive 90 degree bends separated by 1 mm was investigated. The flow patterns obtained were compared with previous works done for conventional, similar and micro sized channels.

In the flow ranges considered, slug, stratified wavy, wavy, annular and churn are the main flow patterns observed. Introducing a mixing area before the entrance to the test section created a well developed churn flow at high liquid and gas flow rates. It also stopped the liquid film from being completely swept away from the "right/lower" wall of the channel at low liquid and high gas flow rates (the gas enter through the "right/lower" branch).

The flow patterns are in good agreement with the maps done for similar size channel by Triplett et al. (1999) and for micro size channel by Serizawa et al. (2002), even though the flow rate areas did not exactly overlap. However, the map did not agree well with the work of Mandhane et al. (1974) for conventional size channels, since the effect of gravity has created more stratified flow in the conventional channels in much of the flow rate areas we covered. Comparison of the values of the Bond numbers, Weber numbers and Capillary numbers for the two flows indicates that the effect of gravitational force is much less significant in this case. Instead, the effect of surface tension is dominant. The flow in the 90 degree bends created an additional pattern which was not observed up stream of the bends. They created bubbly flow for cases where the deformation on the gas slugs passing the bend is so high that they disintegrate to create new bubbles.

It is generally observed that the flow pattern in 1mm x 1mm cross section channels depends on the interfacial tension, wall roughness, and mixing conditions at the entrance. This can be exploited in application design. Future work should investigate the sensitivity to variations in the inlet conditions of the gas and liquid flow.

Nomenclature

Bo	Bond number [-]
Ca	Capillary number [-]
Co	Confinement number [-]
D	Air diffusivity in water [m^2/s]
D_h	Hydraulic diameter [m]
g	Gravitational acceleration [m/s^2]
Kn	Knudsen number [-]
L	Laplace constant [m]
Pe	Peclet number [-]
Re	Reynolds number [-]
U	Characteristic flow velocity [m/s]
V_{sa}	Superficial velocity of air [m/s]
V_{sw}	Superficial velocity of water [m/s]
We	Weber number [-]
δ	Lattice spacing of water molecules [m]
$\sum$	Eotwös number [-]
λ	Mean free path of air molecules [m]
ρ_l	Liquid density [kg/m^3]
ρ_g	Gas density [kg/m^3]
σ	Surface tension [N/m]

References

Angeli, P., and Hewitt, G. F., (2000) *Int. J. Multiphase Flo* , 26, 1117 – 1140.

Badie, S., Hale, C. P., Lawerence, C. J., and Hewitt, G. F., (2000) *Int. J. Multiphase Flow* , 26, 1525 – 1543.

Brauner, N., and Moalem-Maron, D., (1992) *Int. Commun. Heat Mass Transfer* , 19, 29 – 39.

Brutin, D., and Tadrist, L., (2004) *Int. J. Heat Mass Transfer* , 47, 2365 – 2377.

Cheng, L., and Mewes, D., (2006) *Int. J. Multiphase Flow* , 32, 183 – 207.

Faghri, M., and Sundén, B., (2004) *Heat and Fluid Flow in Microscale and Nanoscale Structures*. WIT Press, Boston.

Fukano, T., Kariyasaki, A., (1993) *Nuclear Eng. Design*, 141, 59 – 68.

Hestroni, G., Mosyak, A., Pogrebnyak, E., and Yarin, L. P., (2005*) Int. J. Heat Mass Transfer* , 48, 1982 – 1998.

Kandlikar, S. G., (2002) *Exp. Thermal and fluid Science*, 26, 389 – 407.

Kew, P. A., and Cornwell, K., (1997) *Appl. Thermal Eng.*, 17, 707 – 715.

Klank, H., Kutter, J. P., and Geschke, O., (2002) *Lab on a Chip***, 2, 242 – 246.

Mandhane, J. M., Gregory, G. A., and Aziz, K., (1974) *Int. J. Multiphase Flow*, 1, 537 – 553.

Serizawa, A., Feng, Z., and Kawara, Z., (2002) *Exp. Thermal Fluid Science*, 26, 703 – 714.

Triplett, K. A., Ghiaasiaan, S. M., Abdei-Khalik, S. I., and Sadowski, D. L., (1999) *Int. J. Multiphase Flow*, 25, 377 – 394.

Wölk, G., Dreyer, M. and Rath, H. J., (2000) *Int. J. Multiphase Flow*, 26, 1037 – 1061.